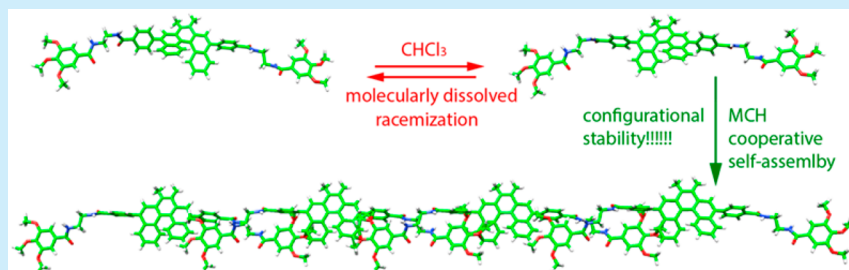


# Supramolecular Polymerization of [5]Helicenes. Consequences of Self-Assembly on Configurational Stability

Jorge S. Valera, Rafael Gómez, and Luis Sánchez\*<sup>✉</sup>

Departamento de Química Orgánica I, Facultad de Ciencias Químicas, Universidad Complutense de Madrid, 28040 Madrid, Spain

**S** Supporting Information



**ABSTRACT:** The supramolecular polymerization of [5]helicenes **1** and **2** is investigated. The self-assembly of these helicenes proceeds by the operation of H-bonding interactions with a negligible participation of  $\pi$ -stacking. The enantiopurity of the sample has a dramatic effect on the supramolecular polymerization mechanism since it reverts the isodesmic mechanism for the racemic mixture to a cooperative one for the enantioenriched sample. Noticeably, the formation of supramolecular polymers efficiently increases the configurational stability of 1,14-unsubstituted [5]helicenes.

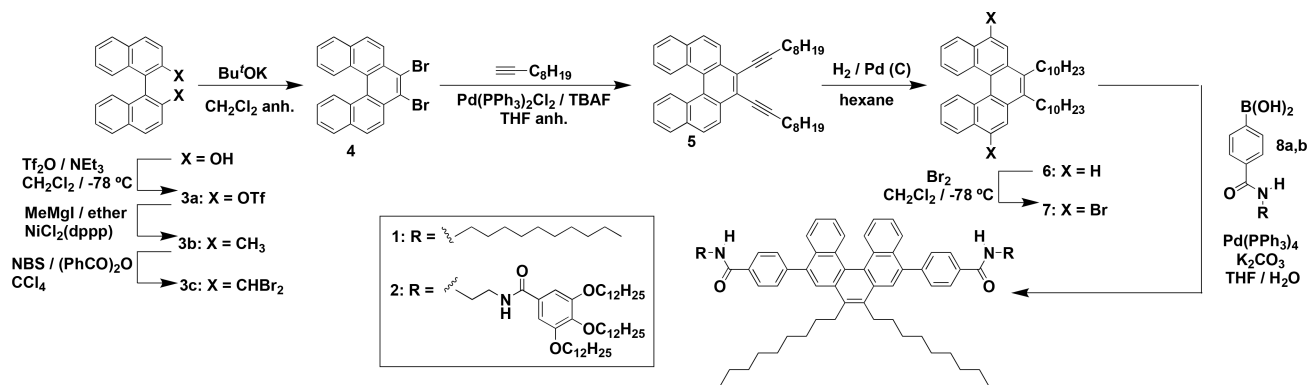
Polyaromatic hydrocarbons (PAHs) are carbon-rich organic compounds showing exciting optical and electronic properties that ensure exploitation in leading scientific and technologic research fields.<sup>1</sup> [*n*]Helicenes, the ortho-fused specimens of PAHs in which  $n \geq 4$ , are currently utilized in enantioselective catalysis,<sup>2</sup> sensing,<sup>3</sup> and as scaffolds to build up distorted nanographene or nanoribbons.<sup>4</sup> From a structural point of view, [*n*]helicenes exhibit a twisted geometry imposed by the steric hindrance between the terminal aromatic rings. The unfavorable steric interaction between these rings generates helical conformation of the  $\pi$ -conjugated system and, consequently, two possible enantiomers in molecules that lack any stereogenic center.<sup>5</sup> However, the configurational stability of [*n*]helicenes strongly depends on the number of aromatic rings. Thus, [4]helicenes are configurationally unstable and can be enantiopurely isolated at room temperature only by decorating their 1 and 12 positions with different substituents.<sup>6</sup> On the other hand, those [*n*]helicenes in which  $n \geq 6$  are configurationally stable with Gibbs activation energy of enantiomerization ( $\Delta G^\ddagger(T)$ ) larger than 40 kcal mol<sup>-1</sup>.<sup>7</sup> More interesting are the stereodynamic features of [5]helicenes since these scaffolds are flexible enough to show an ample range of  $\Delta G^\ddagger(T)$  values, depending on the substitution at the fjord region.<sup>8</sup> The substitution in one or two of these 1 or 14 positions results in highly stable enantiomers with a large resistance to racemization.

Herein, we report on the supramolecular polymerization<sup>9</sup> of 5,7,8,10-tetrasubstituted [5]helicenes (compounds **1** and **2** in Scheme 1) as a very useful strategy to increase the configurational stability of [5]helicenes. We investigated the self-assembly in solution of both the racemic and enantioen-

riched forms of the [5]helicenes **1** and **2**. The experimental data show that only the formation of a quadruple array of H-bonds between the amide functional groups of **2** allows the efficient noncovalent interaction in apolar solvents. At the same time, enantiopurity plays a crucial role in the supramolecular polymerization mechanism being isodesmic for the racemic mixture and cooperative for the enantioenriched [5]helicene. Finally, we demonstrate that the formation of supramolecular polymers from the enantioenriched isomer noticeably increases the configurational stability of the [5]helicene **2**. The results presented in this manuscript provide new tools for achieving configurationally stable [5]helicenes and demonstrate the enormous potential of supramolecular polymerization to accomplish new functionalities for these attractive molecules.

To achieve soluble self-assembling units that allow investigation of the supramolecular polymerization of [5]helicenes in solution, the decoration of the aromatic backbone with long alkyl tails is necessary. We have followed previously reported multistep synthetic protocols making use of BINOL as starting material and involving a benzylic coupling as a key step to construct the [5]helicene moiety.<sup>10</sup> Reacting 7,8-dibromo[5]helicene **4**<sup>10b</sup> by a Sonogashira cross-coupling reaction catalyzed by Pd with 1-decyne gives **5**. The catalytic hydrogenation of alkyne **5**, followed by the regioselective aromatic bromination at the 5 and 10 positions yields the highly soluble dibromo[5]helicene **7**. A final Suzuki reaction of **7** with the carbamoylphenyl boronic acid **8a**<sup>11</sup> or **8b**<sup>11</sup> affords

**Received:** February 15, 2018

Scheme 1. Synthesis of the 5,7,8,10-Tetrasubstituted [5]Helicenes **1** and **2**

the dicarboxamide **1** or the tetracarboxamide **2**, respectively (Scheme 1).  $^1\text{H}$  NMR,  $^{13}\text{C}$  NMR, and FTIR spectroscopy and MALDI-TOF spectrometry have been used to corroborate the chemical structure of all new described compounds (see the Supporting Information).

The self-assembly of  $[n]$ helicenes, especially for the case of enantiopure specimens,<sup>12</sup> has been amply investigated on surfaces with the examples reported in solution being scarce.<sup>13</sup> To disclose the noncovalent forces operating in the supramolecular polymerization of helicenes **1** and **2**, we have investigated the self-assembly in solution of [5]helicene **1**, endowed with two amides, by using concentration-dependent  $^1\text{H}$  NMR and variable-temperature (VT) UV-vis experiments. In these experiments, a negligible shift of all aromatic and amide protons is visible (Figure S1). In addition, VT-UV-vis experiments in a very apolar solvent, like methylcyclohexane (MCH), show no crossing points between the spectra registered at 20 and 90 °C at concentrations as high as 100  $\mu\text{M}$  (Figure S2). This behavior, a consequence of the lack of intermolecular interactions (i.e., H-bonds between the amide groups and  $\pi$ -stacking of the aromatic units), contrasts with that described for referable dicarboxamides in which the synergy of both H-bonding and  $\pi$ -stacking yields an efficient self-assembly process.<sup>11,14</sup>

Considering the difficulty of  $[n]$ helicenes to interact by  $\pi$ -stacking between the twisted aromatic moieties,<sup>3</sup> we have designed [5]helicene **2** endowed with two 3,4,5-trialkoxy-*N*-alkoxybenzamide units that have been shown to enhance the supramolecular polymerization features of self-assembling molecules.<sup>15</sup> In concentration-dependent  $^1\text{H}$  NMR spectra of **2** in  $\text{CDCl}_3$  as solvent, most of the aromatic resonances experience an unappreciable shift, except the resonances corresponding to the protons at the 6 and 9 positions and the methylene protons of the paraphenic side chains linked to the helicene moiety that slightly shift upfield upon increasing the concentration (Figure S3). More appreciable is the deshielding effect observed for the amide protons upon increasing concentration that implies the operation of H-bonding interactions between the amide groups.<sup>16</sup> Diffusion-ordered spectroscopy (DOSY) NMR experiments at concentrated (20 mM) and diluted conditions (1 mM) confirm the aggregation of **2** since the diffusion of the sample is slower at 20 mM than for the diluted sample (Figure S4).<sup>17</sup> These findings suggest the lack of efficient  $\pi$ -stacking between the aromatic units but the formation of  $\text{N}-\text{H}\cdots\text{O}=\text{C}$  H-bonds between the amide functional groups. Moreover, a rotating-frame Overhauser effect spectroscopy (ROESY) NMR experiment in a

concentrated solution of **2** corroborates that the supramolecular organization of this helicene is only due to the formation of H-bonds between the amides. Thus, only a number of through-space intramolecular coupling signals between the spatially close protons of the molecule are observed (Figure S5).

To disentangle the supramolecular polymerization mechanism of **2**, we have performed VT-UV-vis in MCH as solvent at a total concentration  $c_T = 10 \mu\text{M}$ . At 20 °C, the UV-vis spectrum of **2** shows two maxima at 270 and 324 nm and a shoulder at 370 nm. Heating this solution to 90 °C results in a spectrum bathochromically shifted by only 2 nm and with a crossing point at 320 nm (Figure S6a). This behavior implies the operation of a self-assembly process in which the  $\pi$ -stacking of the aromatic units is not relevant, in agreement with that previously reported for closely related [5]helicenes.<sup>13b</sup> Plotting the variation of the absorbance at 339 nm versus temperature shows a nonlinear trend that cannot be accurately fitted to the equilibrium (EQ) model described for one-component supramolecular polymerization (Figure S6b).<sup>18</sup> The enantiomerization of the helicene core, concomitant to the disassembly of the aggregates formed by **2**, could account for this inaccurate fitting. To circumvent this drawback, we have studied the supramolecular polymerization mechanism by using the solvent-denaturation (SD) model.<sup>19</sup> This model considers the supramolecular polymerization as a balance between the effect of mixing a good and a bad solvent that favors the solvation or the aggregation of the monomeric species, respectively. To perform this study, solutions of **2** in MCH as bad solvent and in  $\text{CHCl}_3$  as good solvent are mixed keeping constant  $c_T$  (Figure S7a). In these experiments, heating the samples is not necessary, thus avoiding the effect of the enantiomerization.<sup>20</sup> Plotting the variation of the degree of aggregation ( $\alpha$ ) versus the molar fraction of the good solvent has been fitted to the SD model to attain the corresponding thermodynamic parameters (Table 1). The sigmoidal curve and the very low derived value for the degree of cooperativity  $\sigma$  (0.35) indicates that the self-assembly of the racemic mixture of **2** is governed by an isodesmic mechanism (Figure S7b).<sup>9</sup>

**Table 1.** Thermodynamic Data for the Supramolecular Polymerization of **2** Derived from the SD Model

	$\Delta G^a$	$\sigma^b$	$K_c^c$	$K_n^c$
(±)- <b>2</b>	-36.1	0.35	$2.1 \times 10^6$	$0.7 \times 10^6$
<i>M</i> - <b>2</b>	-38.5	0.001	$5.6 \times 10^6$	$6.1 \times 10^3$

<sup>a</sup>kJmol<sup>-1</sup>; <sup>b</sup> $\sigma = K_n/K_c$ ; <sup>c</sup>M<sup>-1</sup>

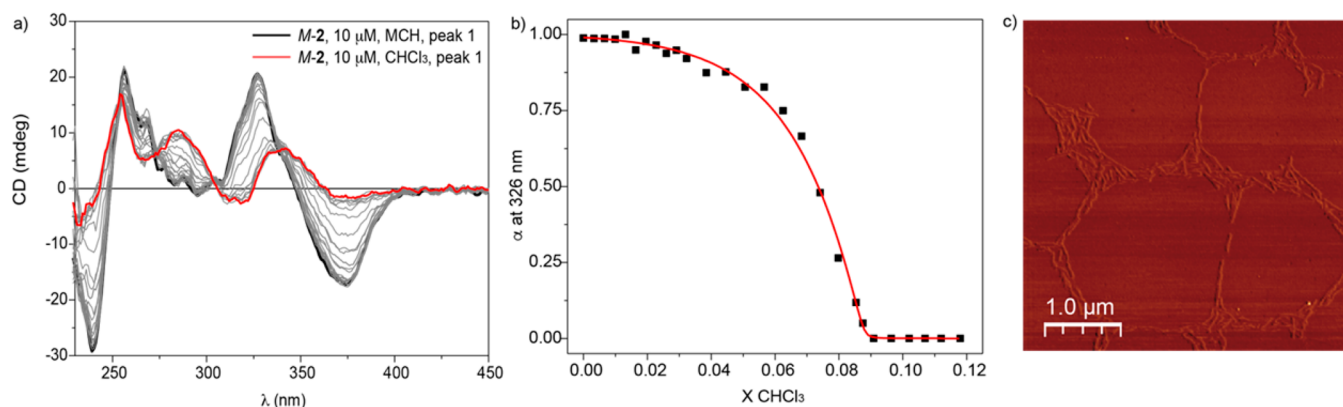


**Figure 1.** CD spectra (a) and denaturation curve (b) of *M*-2 in MCH/CHCl<sub>3</sub> mixtures ( $1 \times 10^{-5}$  M; 298 K). The red line in (b) depicts the fitting to the SD model. (c) AFM phase image of the columnar aggregates formed from *M*-2 (10  $\mu$ M, 298 K, mica as surface).

The racemic mixture of *P* and *M* enantiomers of [5]helicenes **1** and **2** can be separated by chiral HPLC (Figure S8). The effective separation and the absolute configuration of these two enantiomers has been assessed by circular dichroism (CD). Thus, the CD spectrum of the first eluted peak shows a negative band at  $\lambda = 374$  nm and a positive band at  $\lambda = 342$  nm with the second eluted peak showing a mirror CD spectra (Figure S9b). This CD pattern is indicative of a *M* absolute configuration for the first eluted enantiomer and a *P* absolute configuration for the second eluted fraction.<sup>3</sup> The dissimilar spectra of **2** in CHCl<sub>3</sub> and in MCH allows deriving all the thermodynamic parameters without heating by using the SD method (Figure 1). In the case of the *M*-enantiomer of **2** (*M*-2), the denaturation curve is clearly nonsigmoidal in shape diagnostic of a cooperative supramolecular polymerization mechanism. Thus, the elongation ( $K_e$ ) and nucleation ( $K_n$ ) constants, as well as the degree of cooperativity  $\sigma$ , depict a completely different mechanistic scenario upon enantiomeric separation (Table 1).

The dissimilar supramolecular polymerization mechanism between the racemic mixture and the *M* enantiomer also has consequences in the different morphology of the supramolecular polymers formed upon self-assembly of **2**. In the case of the racemic mixture, atomic force microscopy (AFM) of a 10  $\mu$ M solution in MCH onto mica as the surface shows the formation of amorphous agglomerates (Figure S10a). However, *M*-2 forms intertwined rodlike aggregates of 3.5 nm height (Figure 1c and Figures S10b and S10c).

During the investigation of the self-assembly of **2** in MCH, we noticed the configurational stability of the sample that retains the same dichroic pattern upon several weeks (Figure S11). Very recently, the configurational stability of [5]helicenes has been related to the number and size of the substituents at the fjord region that strongly conditions the torsional angle  $\theta$  of the aromatic backbone.<sup>8</sup> Compound **2**, which is not decorated with substituents at the fjord region, self-assembles by the formation of H-bonding interactions between the amide groups but without efficient  $\pi$ -stacking of the aromatic units, which should not affect to the value of  $\theta$ . Consequently, the  $\Delta G^\ddagger(T)$  should be similar in the aggregated or molecularly dissolved state. However, the solvation of **2** in CHCl<sub>3</sub>, a good solvent that favors the disassembly of the supramolecular polymer, yields configurationally unstable samples that rapidly racemize. We have calculated the value of  $\Delta G^\ddagger(T)$  for **2** in the molecularly dissolved state by utilizing the changes of the CD spectra against time and the Eyring equation (see the Supporting

Information and Figure S12).<sup>21</sup> In these experimental conditions,  $\Delta G^\ddagger(328)$  has been calculated as  $23 \pm 2$  kcal mol<sup>-1</sup>, in very good agreement with the reported data for 1,14-unsubstituted [5]helicenes ( $\sim 25$  kcal mol<sup>-1</sup>).<sup>3,8</sup> Interestingly, heating a solution of **2** in MCH, at  $c_T = 10$   $\mu$ M and at 328 K shows no racemization in the same range of time, thus demonstrating the enhanced configurational stability achieved by the supramolecular polymerization (Figure S12b). A further proof of the influence of supramolecular polymerization on the configurational stability is that a solution of the *P* enantiomer of **1** (*P*-1) in MCH also experiences racemization with a very similar value of  $\Delta G^\ddagger(T)$  ( $\Delta G^\ddagger(328) = 24$  kcal mol<sup>-1</sup>) (Figure S13). Finally, in order to prove that the solvent MCH is not responsible for the improved configurational stability of the *M*-2 supramolecular polymer, we have registered CD spectra of *M*-2 at  $c_T = 10$   $\mu$ M at different temperatures (Figure 2). Plotting

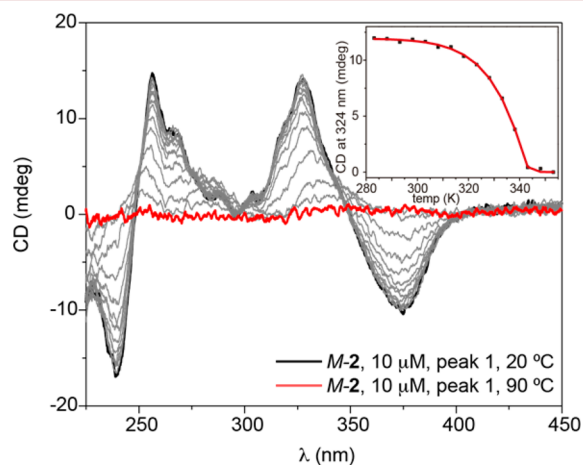


**Figure 2.** CD spectra of *M*-2 at 20 and 90  $^{\circ}$ C (MCH,  $c_T = 10$   $\mu$ M). The inset shows the nonsigmoidal trend of the variation of the dichroic response at 324 nm versus temperature. The red line in the inset corresponds to the fitting to the EQ model.

the variation of the dichroic response versus temperature results in a nonsigmoidal curve that fits to a nucleation–elongation (or cooperative) model.<sup>9</sup> This VT-CD study shows that the intensity of the dichroic bands decrease upon increasing temperature, and it is completely canceled at 70  $^{\circ}$ C. At this temperature ( $T_c$ ), the elongation regime changes to the nucleation one, and as soon as the supramolecular polymer is

disassembled, the racemization of the sample takes place (inset in Figure 2).

To summarize, the results presented herein describe the supramolecular polymerization and the noncovalent forces operating in the self-assembly of 1,14-unsubstituted [5]-helicenes. The studies presented in the manuscript demonstrate that the enantiopurity of the sample changes the supramolecular polymerization mechanism that switches from an isodesmic one, for the racemic mixture, to a cooperative one for the enantioenriched *M*-2. More importantly, we demonstrate that, due to the organized self-assembly of these unsubstituted curved PAHs at the fjord region, they are conformationally stable, thus demonstrating the enormous potential of supramolecular polymerization to accomplish configurational stability of [5]helicenes.

## ■ ASSOCIATED CONTENT

### Supporting Information

The Supporting Information is available free of charge on the ACS Publications website at DOI: [10.1021/acs.orglett.8b00565](https://doi.org/10.1021/acs.orglett.8b00565).

Supplementary figures, experimental procedures, derivation of  $\Delta G^\ddagger(T)$ , and complete characterization (PDF)

## ■ AUTHOR INFORMATION

### Corresponding Author

\*E-mail: [lusamar@quim.ucm.es](mailto:lusamar@quim.ucm.es).

### ORCID

Luis Sánchez: [0000-0001-7867-8522](https://orcid.org/0000-0001-7867-8522)

### Notes

The authors declare no competing financial interest.

## ■ ACKNOWLEDGMENTS

Financial support by the MINECO of Spain (CTQ2014-53046-P and CTQ2017-82706-P) and the Comunidad de Madrid (NanoBIOSOMA, S2013/MIT-2807) is acknowledged. J.S.V. thanks the MINECO for a predoctoral FPI grant.

## ■ REFERENCES

- (1) (a) Wu, J.; Pisula, W.; Müllen, K. *Chem. Rev.* **2007**, *107*, 718. (b) Seyler, H.; Purushothaman, B.; Jones, D. J.; Holmes, A. B.; Wong, W. W. H. *Pure Appl. Chem.* **2012**, *84*, 1047. (c) Müllen, K.; Rabe, J. P. *Acc. Chem. Res.* **2008**, *41*, 511.
- (2) (a) Aillard, P.; Voituriez, A.; Marinetti, A. *Dalton Trans.* **2014**, 43, 15263. (b) Narcis, M. J.; Takenaka, N. *Eur. J. Org. Chem.* **2014**, 2014, 21. (c) Peng, Z.; Takenaka, N. *Chem. Rec.* **2013**, *13*, 28.
- (3) Chen, C.-F.; Shen, Y. *Helicene Chemistry: From Synthesis to Applications*; Springer: Heidelberg, 2017.
- (4) (a) Hu, Y.; Wang, X.-Y.; Peng, P.-X.; Wang, X.-C.; Cao, X.-Y.; Feng, X.; Müllen, K.; Narita, A. *Angew. Chem., Int. Ed.* **2017**, *56*, 3374. (b) Fujikawa, T.; Segawa, Y.; Itami, K. *J. Am. Chem. Soc.* **2016**, *138*, 3587. (c) Ravat, P.; Šolomek, T.; Rickhaus, M.; Häussinger, D.; Neuburger, M.; Baumgarten, M.; Juriček, M. *Angew. Chem., Int. Ed.* **2016**, *55*, 1183.
- (5) (a) Rickhaus, M.; Mayor, M.; Juriček, M. *Chem. Soc. Rev.* **2016**, *45*, 1542.
- (6) (a) Kemp, C. M.; Mason, S. F. *Chem. Commun.* **1965**, 559. (b) Newman, M. S.; Mentzer, R. G.; Slomp, G. *J. Am. Chem. Soc.* **1963**, *85*, 4018. (c) Shigeno, M.; Kushida, Y.; Yamaguchi, M. *Chem. Commun.* **2016**, *52*, 4955.
- (7) (a) Martin, R. H.; Marchant, M. J. *Tetrahedron Lett.* **1972**, *13*, 3707. (b) Grimme, S.; Peyerimhoff, S. D. *Chem. Phys.* **1996**, *204*, 411.
- (c) Janke, R. H.; Haufe, G.; Würthwein, E.-U.; Borkent, J. H. *J. Am. Chem. Soc.* **1996**, *118*, 6031. (d) Martin, R. H.; Marchant, M. J. *Tetrahedron* **1974**, *30*, 347.
- (8) Ravat, P.; Hinkelmann, R.; Steinebrunner, D.; Prescimone, A.; Bodoky, I.; Juriček, M. *Org. Lett.* **2017**, *19*, 3707.
- (9) De Greef, T. F. A.; Smulders, M. M. J.; Wolffs, M.; Schenning, A. P. H. J.; Sijbesma, R. P.; Meijer, E. W. *Chem. Rev.* **2009**, *109*, 5687.
- (10) (a) Ooi, T.; Kameda, M.; Maruoka, K. *J. Am. Chem. Soc.* **2003**, *125*, 5139. (b) Goretta, S.; Tasciotti, C.; Mathieu, S.; Smet, M.; Maes, M.; Chabre, Y. M.; Dehaen, W.; Giasson, R.; Raimundo, J.-M.; Henry, C. R.; Barth, C.; Gingras, M. *Org. Lett.* **2009**, *11*, 3846.
- (11) (a) García, F.; Buendía, J.; Ghosh, S.; Ajayaghosh, A.; Sán chez, L. *Chem. Commun.* **2013**, *49*, 9278. (b) Greciano, E. E.; Sánchez, L. *Chem. - Eur. J.* **2016**, *22*, 13724.
- (12) (a) Ernst, K.-H. *Acc. Chem. Res.* **2016**, *49*, 1182. (b) Cao, H.; Minoia, A.; De Cat, I.; Seibel, J.; Waghray, D.; Li, Z.; Cornil, D.; Mali, K. S.; Lazzaroni, R.; Dehaen, W.; De Feyter, S. *Nanoscale* **2017**, *9*, 18075.
- (13) (a) Kaseyama, T.; Furumi, S.; Zhang, X.; Tanaka, K.; Takeuchi, M. *Angew. Chem., Int. Ed.* **2011**, *50*, 3684. (b) Hirose, T.; Ito, N.; Kubo, H.; Sato, T.; Matsuda, K. *J. Mater. Chem. C* **2016**, *4*, 2811.
- (14) Buendía, J.; Calbo, J.; Ortí, E.; Sánchez, L. *Small* **2017**, *13*, 1603880.
- (15) Valera, J. S.; Gómez, R.; Sánchez, L. *Small* **2018**, *14*, 1702437.
- (16) (a) García, F.; Sánchez, L. *J. Am. Chem. Soc.* **2012**, *134*, 734. (b) García, F.; Viruela, P. M.; Matesanz, E.; Ortí, E.; Sánchez, L. *Chem. - Eur. J.* **2011**, *17*, 7755.
- (17) (a) Wong, A.; Ida, R.; Spindler, L.; Wu, G. *J. Am. Chem. Soc.* **2005**, *127*, 6990. (b) Valera, J. S.; Calbo, J.; Gómez, R.; Ortí, E.; Sánchez, L. *Chem. Commun.* **2015**, *51*, 10142.
- (18) Ten Eikelder, H. M. M.; Markvoort, A. J.; de Greef, T. F. A.; Hilbers, P. A. J. *J. Phys. Chem. B* **2012**, *116*, 5291.
- (19) Korevaar, P. A.; Schaefer, C.; de Greef, T. F. A.; Meijer, E. W. *J. Am. Chem. Soc.* **2012**, *134*, 13482.
- (20) Buendía, J.; Greciano, E. E.; Sánchez, L. *J. Org. Chem.* **2015**, *80*, 12444.
- (21) Xie, Z.; Stepanenko, V.; Radacki, K.; Würthner, F. *Chem. - Eur. J.* **2012**, *18*, 7060.